OKU Fen Bilimleri Enstitüsü Dergisi
8(3): 1009-1023, 2025

OKU Journal of The Institute of Science and Technology, 8(3): 1009-1023, 2025

Osmaniye Korkut Ata Üniversitesi Fen Bilimleri Enstitüsü Dergisi

Osmaniye Korkut Ata University Journal of The Institute of Science and Technology

Bandwidth Optimization of an Ultra Wide Band Vivaldi Antenna Design with Its Feed Alignment

Izzet GÜZELKARA[1*], Veli Tayfun KILIC[2]

[1]Abdullah Gul University, Graduate School of Engineering and Science, Electrical and Computer Engineering, Kayseri
[2]Abdullah Gul University, Faculty of Engineering, Electrical and Electronics Engineering, Kayseri

[1]https://orcid.org/0000-0001-5287-4293
[2]https://orcid.org/0000-0001-6806-9053
*Corresponging author: izzet.guzelkara@agu.edu.tr

Research Article

Article History:
Received: 22.07.2024
Acceptedi:30.01.2025
Published Online: 16.06.2025

Keywords:
Vivaldi
Ultra wide band
Microstrip feed

ABSTRACT

Ultra wide band applications such as medical imaging, surveillance or indoor localization require different bandwidths. The different bandwidth requirements often present a challenge in terms of antenna design. In this paper, a wideband Vivaldi antenna which is suitable for UWB systems is presented. The antenna is designed and optimized using a 3D electromagnetic simulation tool. Then, a parametric study is carried out that investigates the effect of microstrip feed on the antennas bandwidth. It is demonstrated that the bandwidth of the antenna can be manipulated by changing the total length and the positioning of the microstrip feed without the need for changing any other antenna parameter.

Ultra Geniş Bant Vivaldi Anten Tasarımında Besleme Hattının Hizalanması ile Bant Genişliği Optimizasyonu

Araştırma Makalesi

Makale Tarihçesi:
Geliş tarihi: 22.07.2024
Kabul tarihi: 30.01.2025
Online yayınlama: 16.06.2025

Anahtar Kelimeler:
Vivaldi
Ultra geniş bant
Mikroşerit besleme

ÖZ

Tıbbi görüntüleme, gözetleme veya iç mekân lokalizasyonu gibi ultra geniş bant uygulamaları farklı bant genişlikleri gerektirir. Farklı bant genişliği gereksinimleri genellikle anten tasarımı açısından zorluk teşkil etmektedir. Bu çalışmada ultra geniş bant sistemlerine uygun geniş bantlı bir Vivaldi anten sunulmaktadır. Anten, 3 boyutlu bir elektromanyetik simülasyon aracı kullanılarak tasarlanmış ve optimize edilmiştir. Daha sonra mikroşerit beslemenin anten bant genişliği üzerindeki etkisinin araştırıldığı parametrik bir çalışma yapılmıştır. Antenin bant genişliğinin, başka herhangi bir anten parametresini değiştirmeye gerek kalmadan, mikroşerit beslemenin toplam uzunluğu ve konumu değiştirilerek değiştirilebileceği gösterilmiştir.

To Cite: Güzelkara I., Kılıc VT. Bandwidth Optimization of an Ultra Wide Band Vivaldi Antenna Design with Its Feed Alignment. Osmaniye Korkut Ata Üniversitesi Fen Bilimleri Enstitüsü Dergisi 2025; 8(3): 1009-1023.

1. Introduction

Ultra-wideband (UWB) systems have been gaining interest in recent years due to the increasing popularity of applications that require spatial awareness such as indoor localization, secure connection, asset tracking, medical monitoring and imaging, and ranging (Paulson et al., 2005; D'Amico et al., 2010; Allebes et al., 2021; G. Singh et al., 2021; Song et al., 2023). UWB antennas are an essential part of the UWB systems and they are widely being researched (Valderas et al., 2010; Shantz, 2015; Saeidi et al., 2019; Kumar et al., 2022). To comply with the system requirements, UWB antennas must possess certain features. These features include operating in a wide spectrum, having a good impedance matching and a wide instantaneous bandwidth (Chang, 2008). Federal Communications Commission (FCC) defines UWB bandwidth as the frequency band bounded by the points that are 10 dB below the highest emission radiated by a complete transmission system including the antennas (Federal Communications Commission, 2002). Furthermore, according to FCC, an UWB transmitter should have a fractional bandwidth equal to or greater than 0.2 or have an operating bandwidth equal to or greater than 500 MHz, regardless of the fractional bandwidth. The fractional bandwidth of a system can be found by Equation 1.

$$\text{Fractional Bandwidth} = \frac{2(f_H - f_L)}{f_H + f_L} \tag{1}$$

where f_H is the highest frequency in the band and f_L is the lowest frequency.

In addition to the requirements mentioned above, the frequencies in which a UWB system operates vary depending on the application. For example, FCC mandates that the bandwidth of UWB surveillance systems should be between 1.99 and 10.6 GHz, while the bandwidth for UWB medical imaging systems must be contained between 3.1 to 10.6 GHz (Breed, 2005). Selecting an antenna that can comply with the requirements mentioned above over the frequency range extending from 1.99 till 10.6 GHz is extremely important when designing an UWB system. First introduced by P. Gibson in 1979 and has been improved since, Vivaldi antennas are a natural choice for UWB systems thanks to their wide bandwidth, high directivity, and low cross polarization (Gibson, 1979; Kahar et al., 2015; Singh et al., 2023). Because of their aperiodic continuously scaled structure, Vivaldi antennas have theoretically unlimited instantaneous bandwidth, which gives them an edge in UWB systems. However, in practice, the bandwidth of most UWB antennas is limited by the bandwidth of the feed network being used.

There are a few studies in the literature that investigate the effect of the feed network on antenna performance (Shafieha et al., 2008; Coburn, 2019; Khusna et al., 2019). In their work Khusna et al. (2019) analyze the effect of the microstrip feed lines in rectangular, shell and circular patterns on the antenna performance. Similarly, Shafieha et al. (2008) examine the microstrip feed structure having a shell pattern and several parameters related to such feed structure. The authors showed that the longitudinal and latitudinal displacement of the radial stub, stub angle and stub offset angle have important effects on the antennas cutoff frequencies and reflection loss. These works provide valuable insights regarding the importance of the feed structure on Vivaldi antenna performance. However, to the best of our knowledge, the effect of rectangular microstrip feed on the bandwidth of Vivaldi antennas has not been documented in detail. In this paper, we propose a Vivaldi antenna that is suitable for UWB applications, whose bandwidth can be tuned by changing the parameters and the positioning of the feed structure. The main contributions of this paper are

- filling the aforementioned gap in the literature,
- demonstrating bandwidth optimization with feed alignment,

- providing a layout for Vivaldi antenna design procedure, and
- forming a basis for future research.

The remainder of the paper is divided into 3 sections, in which the proposed antenna design is discussed, simulation results are given and evaluated, and finally, conclusions are drawn.

2. Antenna Design

Vivaldi antennas are a type of end-fire, exponentially tapered slot antennas. A Vivaldi antenna radiates on a metalized dielectric substrate with an exponentially tapered slot and is excited with a microstrip line on the back side of the substrate. Figure 1 shows the structure of the proposed Vivaldi antenna with a rectangular feed line and its geometrical parameters from top, bottom and perspective views. In subfigures (a) and (c) the metal parts made of copper on the top side are painted in yellow and the feed line on the back side is marked with dotted lines, whereas in subfigure (b) the feed line is shown in red. In the past, several studies were carried out to determine how the design parameters affect the antenna performance (Shafieha et al., 2008; Rana et al., 2018). These studies show that the minimum operating frequency of the antenna is inversely proportional to its length and the width of its aperture (Hamzah and Othman, 2011). In theory, the maximum and the minimum aperture widths, i.e., w_{max} and w_{min}, can be calculated as in Equations 2 and 3, respectively,

$$w_{max} = \frac{c}{2f_{min}\sqrt{\varepsilon_r}} \tag{2}$$

$$w_{min} = \frac{c}{f_c\sqrt{\varepsilon_r}} \tag{3}$$

where c is the speed of light, f_{min} is the minimum frequency at which the antenna operates and ε_r is the dielectric constant of the substrate. Also, f_c is the center frequency of the antenna band. Based on these equations, a Vivaldi antenna, which has a bandwidth, as defined above, between 3 and 13 GHz was designed, and its parameters were optimized as summarized in Table 1.

Table 1. Antenna parameters

Parameter	**Dimension (mm)**	**Parameter**	**Dimension (mm)**
a	0.5	L_s	11
T	48	d	1
W_{sub}	60	W_m	3
QW_s	4	QW_m	4
Subh	1.57	MS_t	$QW_m + 2a + W_{sub}/2$

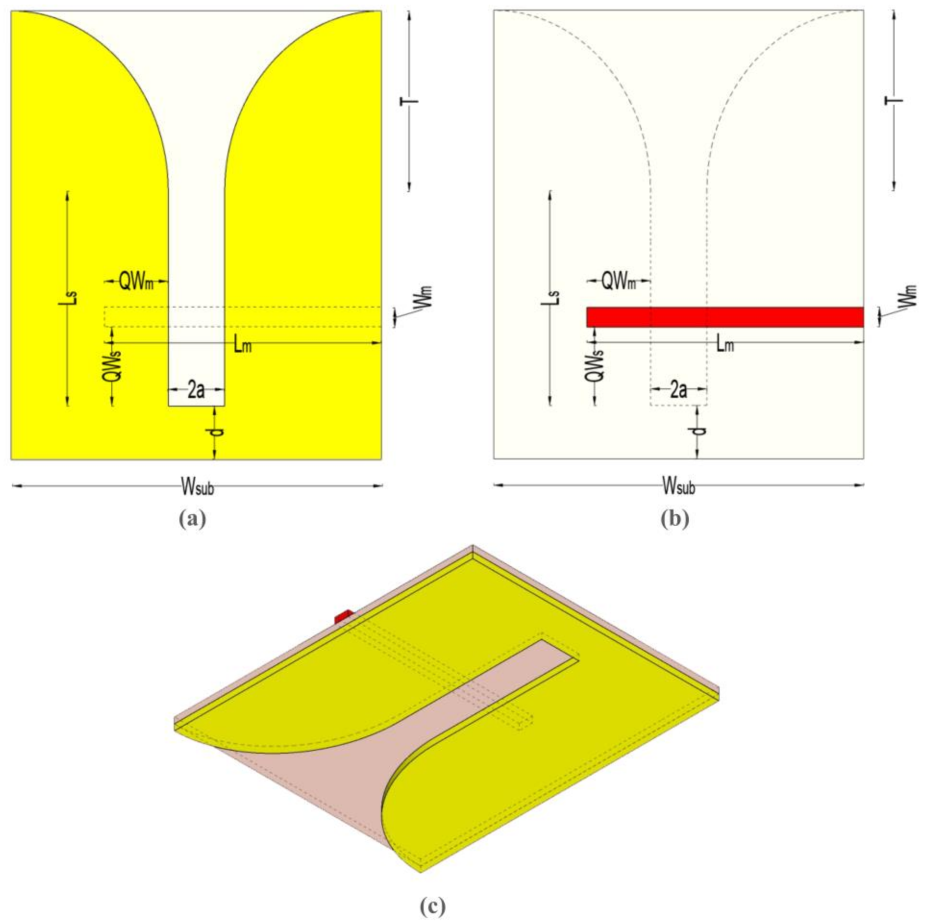

Figure 1. Structure of the proposed antenna and its geometrical parameters from (a) top, (b) bottom and (c) perspective views.

The parameters given in the table are named in coherence with the parameters shown in Figure 1. In the table, the parameter W_{sub} is the width of the FR4 substrate, which is equal to the maximum aperture width calculated by Equation 2. The thickness of the substrate, subh, is 1.57 mm, whereas parameter a is the half width of the linear slot measured from the center of the antenna and its value is 0.5 mm in the designed antenna. The width of the microstrip line, W_m, is chosen as 3 mm to have a 50 Ω impedance matching. Parameters QW_m and QW_s, on the other hand, represent the longitudinal and latitudinal displacements of the microstrip feed starting from the linear slot line. They were initially chosen as the quarter wavelength inside the substrate at the center frequency and were later optimized. L_s is the total length of the linear slot with the offset d valued from the back wall of the antenna. The total length of the tapered flare, T is 48 mm and its profile is determined by Equation 4.

$$y = C_1 e^{rx} + C_2 \tag{4}$$

In the equation, x and y stand for the positions of points on a flare in cartesian coordinates, and r is the opening rate of the flare. Also, C_1 and C_2 are the parameters related to coordinates of the flare's start and end points and are calculated by Equations 5 and 6, respectively,

$$C_1 = \frac{y_2 - y_1}{e^{rx_2} - e^{rx_1}} \tag{5}$$

$$C_2 = \frac{y_1 e^{rx_2} - y_2 e^{rx_1}}{e^{rx_2} - e^{rx_1}} \tag{6}$$

where coordinates (x_1,y_1) and (x_2,y_2) are the start and end points of the flare.

3. Results and Discussion

Once an initial design of the antenna was obtained, the parameters were optimized using a three-dimensional (3D) electromagnetic simulation tool as given in Table 1. The resonance behavior, maximum directivity, and the gain of the antenna were examined. S11 parameter magnitude, i.e., return loss, change of the antenna with frequency calculated in the simulations over the band between 2 GHz and 16 GHz is shown in Figure 2(a). As can be seen from the figure, the antenna has a -10 dB bandwidth, i.e., the S11 parameter is less than or equal to -10 dB, extending from 3.1 to 13.6 GHz. In the figure -10 dB level and the corresponding cutoff frequencies are represented with horizontal and vertical dash-dotted lines, respectively. Although there are some peak points in the S11 trace where the S11 magnitude exceeds -10 dB around the frequencies 3.9 GHz, 7.8 GHz, 9.3 GHz and 10.5 GHz, these excesses are negligibly small. The S11 magnitudes calculated at these frequencies are -9.2 dB, -9.5 dB, -9.7 dB and -9.3 dB, respectively. Moreover, the realized gain of the antenna over the band between 2 GHz and 16 GHz calculated in the simulations is depicted in Figure 2(b). In the figure, it is seen that the realized gain varies between 0.8 and 5.5 dBi over the band spanning from 3.1 GHz to 13.6 GHz.

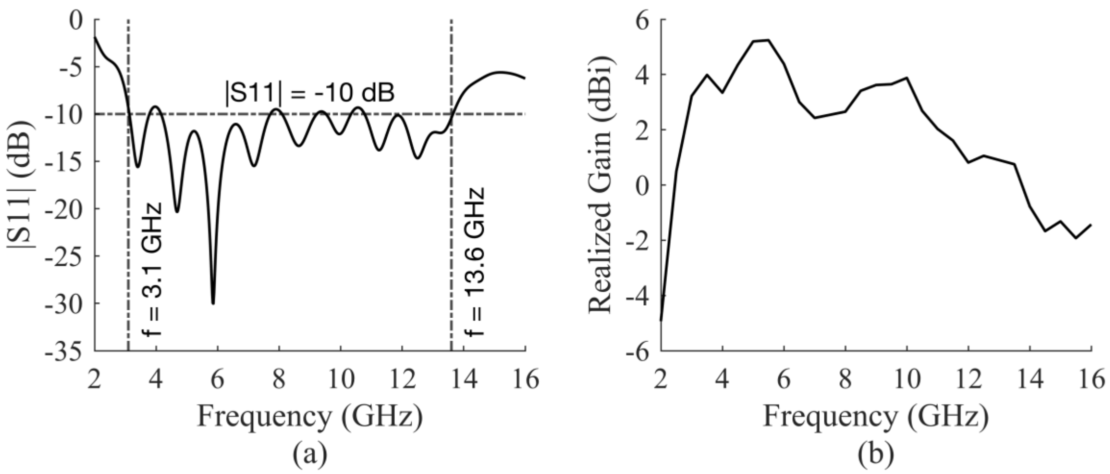

Figure 2. (a) Return loss and, (b) realized gain changes of the optimized antenna with frequency calculated in the simulations over the band between 2 and 16 GHz.

After the optimization, a parametric sweep was carried out on the microstrip feed, where the effects of the feed network parameters QW_s and QW_m that correspond to the position of the feed with respect to the linear slot start point and length of the feed exceeding the linear slot, respectively, on the antenna bandwidth and the gain were observed. As the first step, simulations were obtained for the microstrip feed line with a constant extension length (QW_m) of 4 mm (see Table 1). The microstrip was moved along the linear slot starting from its bottom until 8 mm away from the bottom point with 1 mm increments. In other words, simulations were done for the antenna with a constant QW_m length of 4 mm and different QW_s distances varying from 0 mm to 8 mm. The change in the return loss and the realized gain of the antenna as the microstrip is moved along the aperture axis is shown in Figure 3.

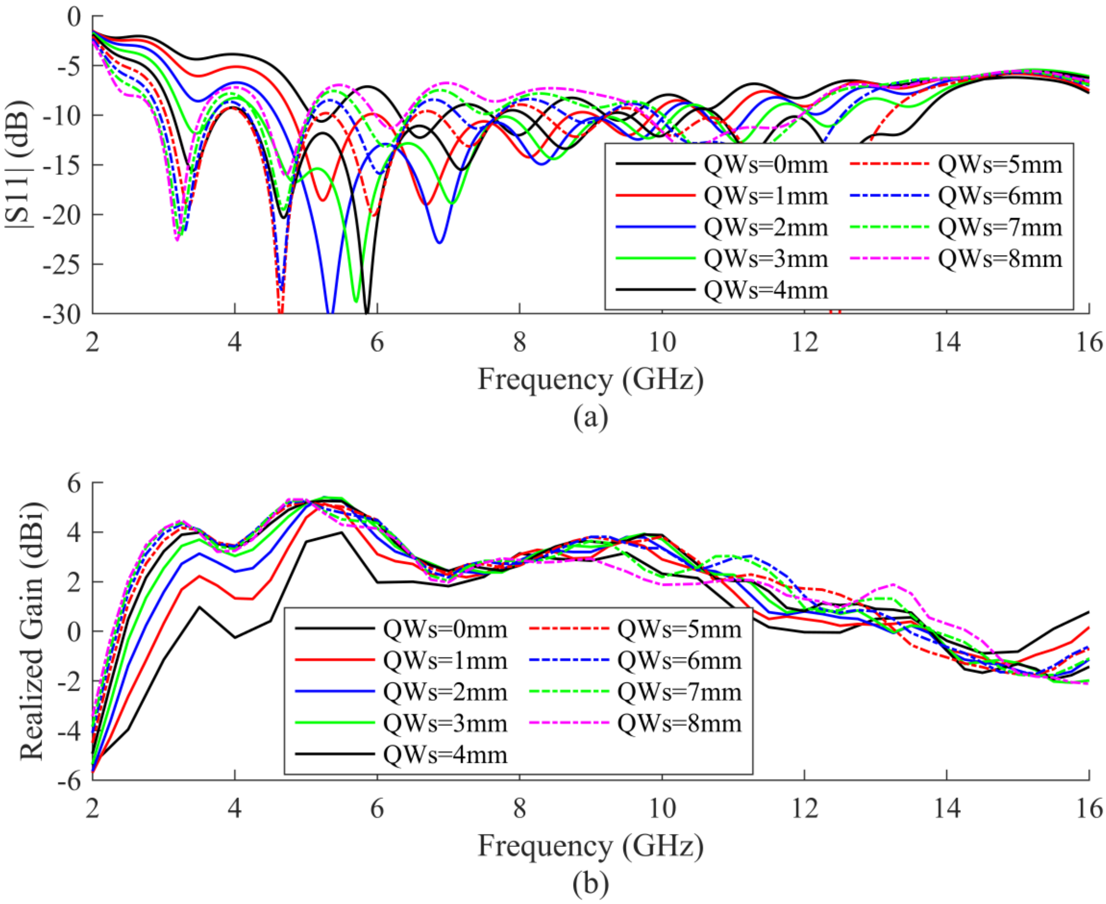

Figure 3. (a) Return loss and, (b) realized gain changes of the designed antenna with frequency calculated in the simulations over the band between 2 and 16 GHz for constant QWm = 4 mm exceed length and different QWs distances.

It is seen from the figure that when the total length of the microstrip is kept constant, moving its position from the bottom of the linear slot until a certain distance (QW_s = 4 mm) increases the total bandwidth of the antenna such that the lower frequency limit of the band shifts to lower frequencies and the upper frequency limit of the band shifts to higher frequencies. On the other hand, as we continue to move the microstrip along the aperture both the lower and the upper limits of the band of the antenna shift to lower frequencies while the total bandwidth is mostly maintained at first and then it decreases. Furthermore, Figure 3(b) shows that the realized gain of the antenna improves as the QW_s distance increases. The lower and upper cutoff frequency shifts and the bandwidth change of the antenna with constant QW_m = 4 mm and different QW_s distances are plotted in Figure 4. In the figure cutoff frequencies and bandwidths corresponding to -10 dB S11 parameter magnitude are considered. In addition, it has been checked to satisfy minimum 500 MHz bandwidth requirement together with peak levels inside the band being lower than -8 dB. Since the S11 magnitude exceeds -10 dB in the interested band a lot for the cases QW_s = 0 and 8 mm, it is not meaningful to define cutoff frequencies and bandwidths for those cases. Consequently, in Figure 4 QWs values in x-axis start and end at 1 mm and 7 mm, respectively.

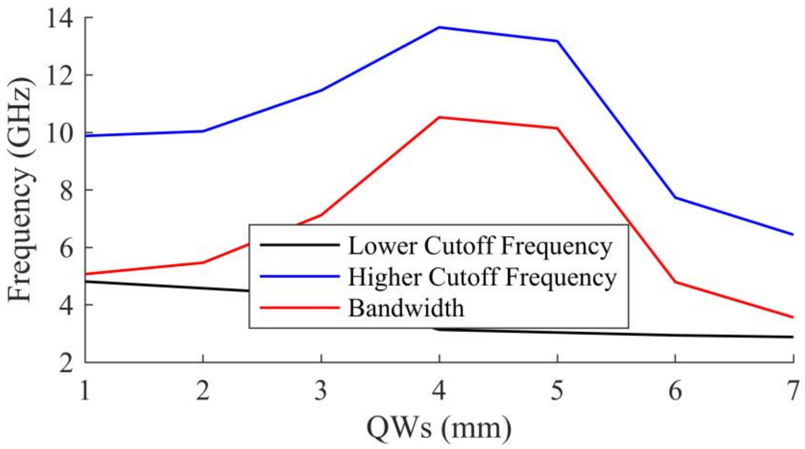

Figure 4. Lower and upper cutoff frequency shifts and bandwidth change of the antenna for constant QWm = 4 mm exceed length and different QWs distances.

Next, simulations were repeated for various exceed lengths of the feed line (QW_m) while keeping the position of the microstrip feed line, i.e., QW_s parameter, constant. Changes in the S11 parameter magnitude and realized gain of the antenna calculated in the simulations over the band between 2 GHz and 16 GHz are shown in Figure 5.

In the figure, it is observed that the lower limit of the antenna band shifts to lower frequencies as the parameter QW_m increases. On the other hand, the upper frequency limit of the antenna band improves until QW_m= 3 mm is reached, and after this point, increasing the length of the microstrip line causes the upper frequency limit to shift to lower frequencies. Moreover, in Figure 5(b) it is seen that as the feed line extends the realized gain of the antenna increases considerably at lower frequencies, i.e., from 2 GHz till 5.5 GHz, while there is no constant increase or decrease at the higher frequencies in the band of the antenna. The lower and upper frequency shifts and the bandwidth change are easily seen in Figure 6 below. In the figure QW_m values in x-axis range between 2 mm and 6 mm because for the cases QW_m = 0, 1 mm, 7 mm, and 8 mm the S11 parameter values are well above -10 dB or exceed this level a lot at many points in the frequency range of interest. Like Figure 4, here while determining cutoff frequencies and bandwidth -10 dB S11 magnitude points are considered. Also, minimum 500 MHz bandwidth requirement together with the maximum peak levels being lower than -8 dB inside the band were checked.

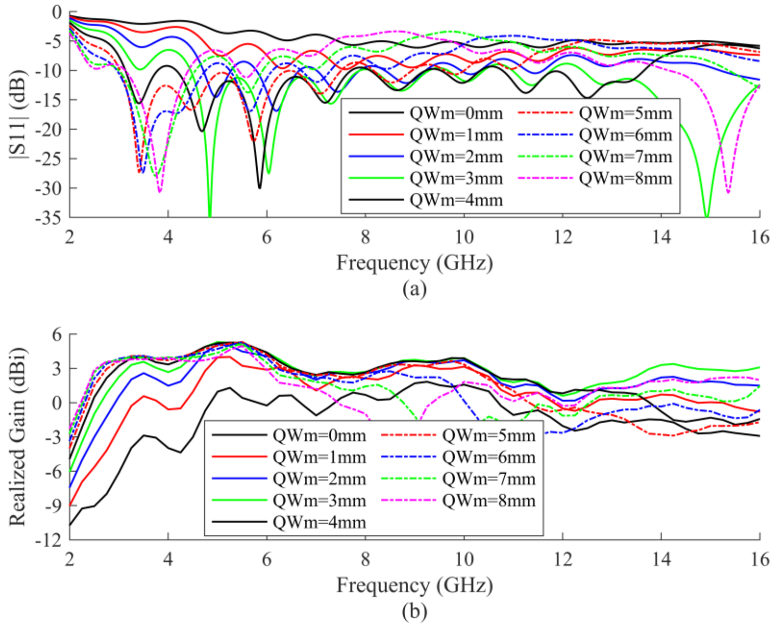

Figure 5. (a) Return loss and, (b) realized gain changes of the designed antenna with frequency calculated in the simulations over the band between 2 and 16 GHz for constant QW_s = 4 mm distance and different QW_m exceed lengths.

After this analysis, simulations were further continued to have a clearer and full understanding of the effects of the feed line parameters on the antenna performance. To this end, simulations were obtained for various feed line lengths and positions that are different from 4 mm. Return loss change of the antenna calculated in the simulations for constant QW_m = 0 mm and 1 mm exceed lengths are shown in Figure 7(a) and Figure 7(b) below, respectively. Here as labeled in the figure QW_s distance is raised from 0 mm until 8 mm with 1 mm steps.

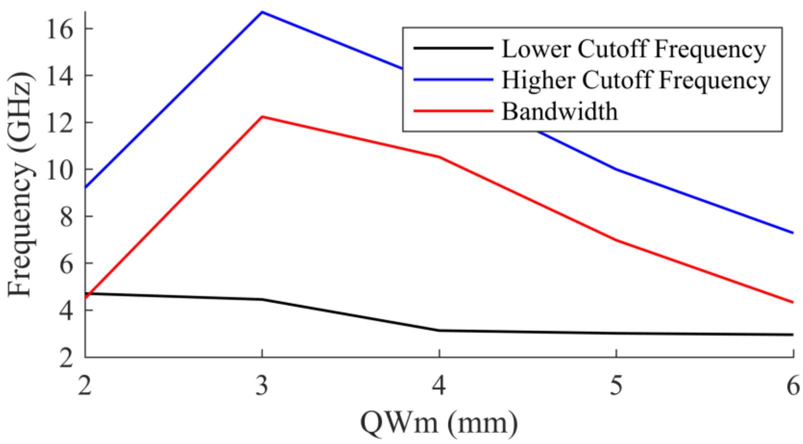

Figure 6. Lower and upper cutoff frequency shifts and bandwidth change of the antenna for constant QW_s = 4 mm distance and different QW_m exceed lengths.

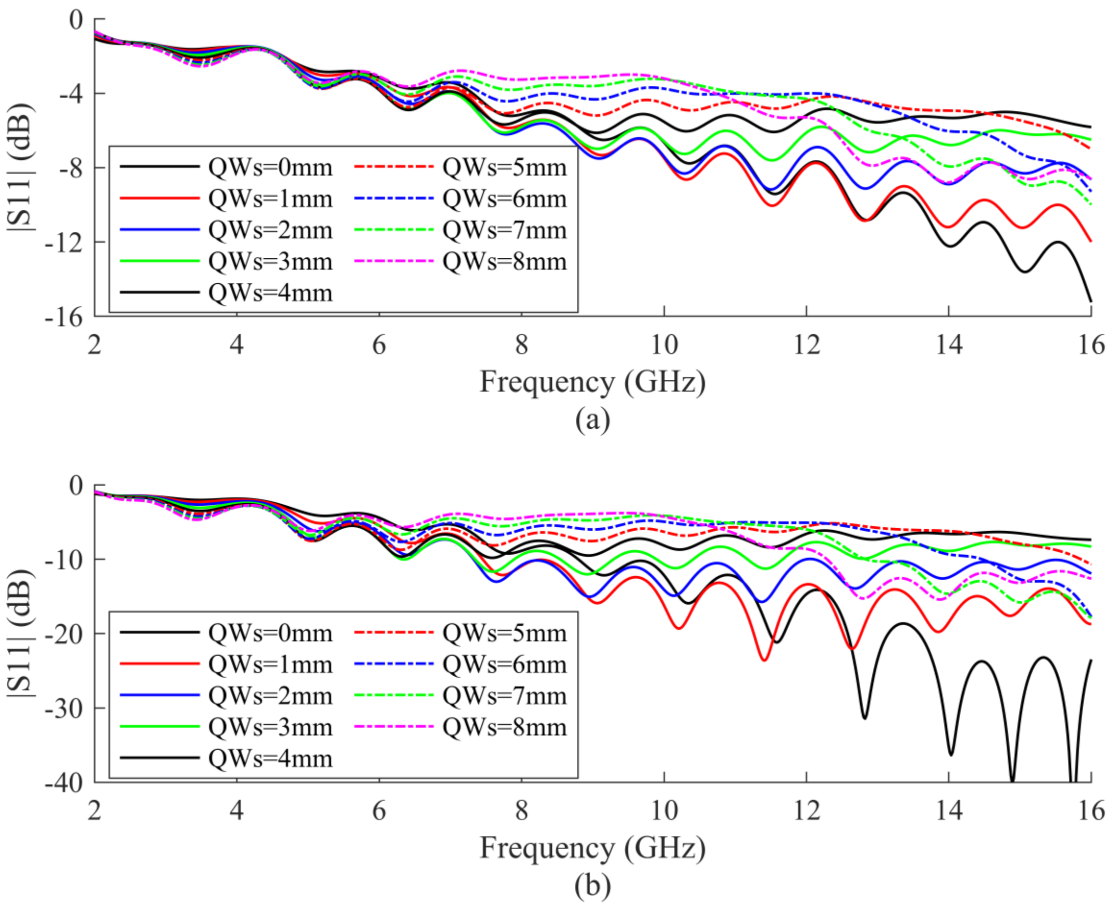

Figure 7. Return loss change of the designed antenna with frequency calculated in the simulations over the band between 2 and 16 GHz for constant (a) QW_m = 0 mm, and (b) QW_m = 1 mm exceed lengths and different QW_s distances.

In the figure, it is seen that for the values of QW_m= 0 mm and 1 mm, the antenna is not able to maintain a -10 dB bandwidth in the desired frequency range. It means, a considerable amount of input power is reflected from the input port of the antenna. Therefore, investigating realized gain of these antennas is not very meaningful. However, when QW_m is incremented to 2 mm, a different resonance behavior of the antenna is observed. Return loss and realized gain changes of the antenna for QW_m exceed length equals to 2 mm are shown in Figure 8 and as seen in subfigure (a), for the cases in which the slot line displacement distance equals to 0 mm, 1 mm, or 2 mm the -10 dB bandwidth of the antenna starts to fall within the desired frequency range, whereas after 2 mm QW_m distance the return loss of the antenna increases, the resonance gets worse and becomes narrower.

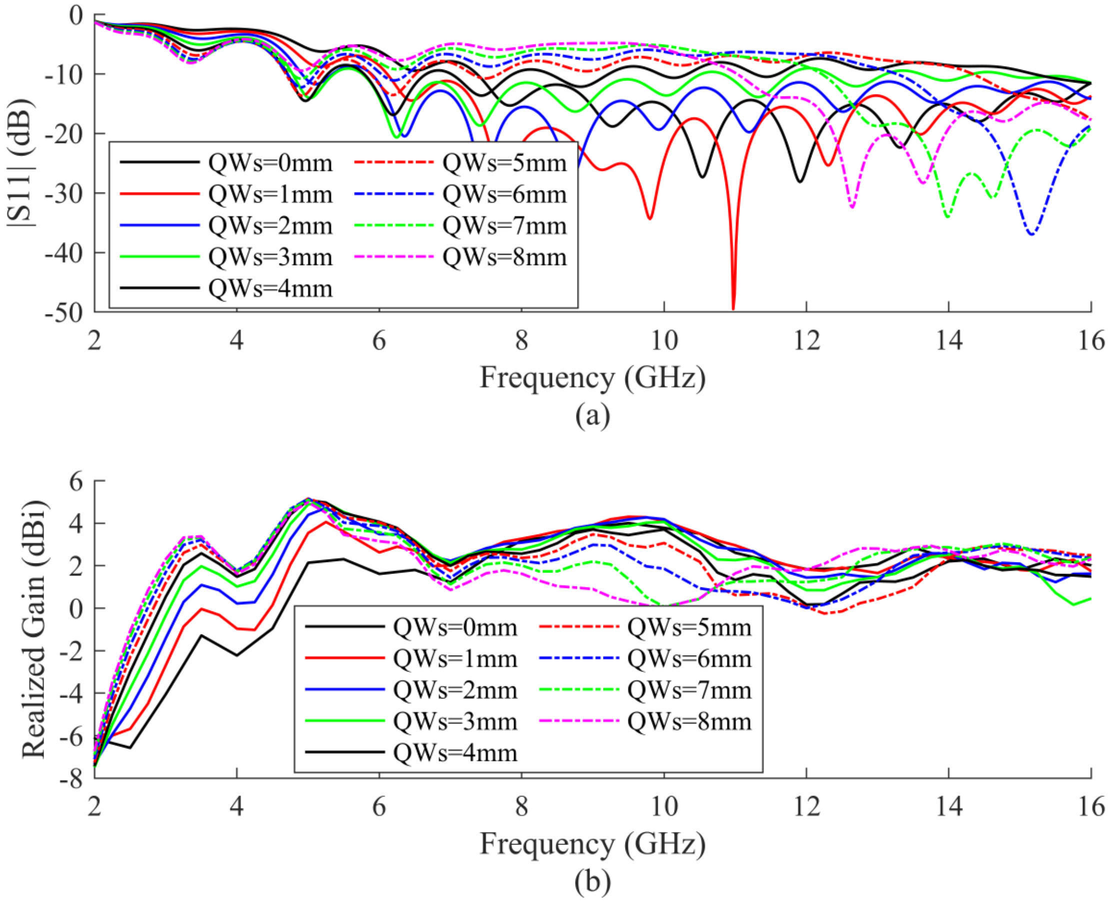

Figure 8. (a) Return loss and, (b) realized gain changes of the designed antenna with frequency calculated in the simulations over the band between 2 and 16 GHz for constant QW_m = 2 mm exceed length and different QW_s distances.

Furthermore, one can see in Figure 8(b) that the realized gain of the antenna improves at the lower frequencies as the parameter QW_s is increased. The enhancement in the gain is obvious between the frequencies 3 GHz and 5 GHz. A similar effect is observed in the resonance behavior and realized gain of the antenna when QW_m exceed length is set to be 3 mm as shown in Figure 9, where return loss and gain variations of the antenna with frequency are plotted for constant QW_m length of 3 mm and different QW_s distances.

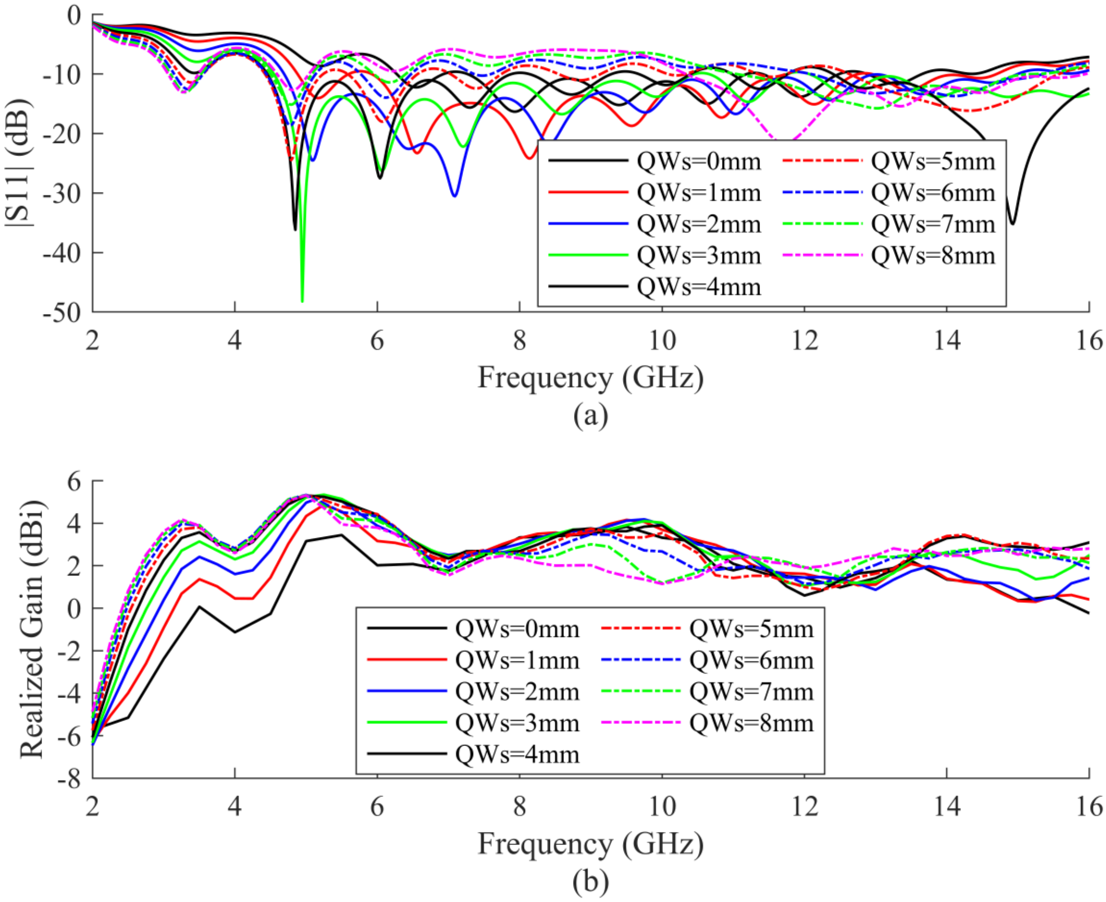

Figure 9. (a) Return loss and, (b) realized gain changes of the designed antenna with frequency calculated in the simulations over the band between 2 and 16 GHz for constant QW_m = 3 mm exceed length and different QWs distances.

Lastly, when QW_m exceed length is increased beyond the initial design of 4 mm to 5 mm, a behavior similar to that observed for the case of QW_m equals to 3 mm is obtained. Return loss and realized gain changes of the antenna for constant 5 mm QW_m exceed length and different QW_s distances are illustrated in Figure 10. As for the case QW_m equals to 3 mm, here, bandwidth of the antenna falls within the desired frequency band when the QW_s distance is small. On the other hand, the resonance gets worse, and the -10 dB bandwidth becomes narrow, i.e. between frequencies 2 GHz and 6 GHz, as QW_s distance increases. In addition, in Figure 10(b) it is observed that the realized gain of the antenna enhances with the enlargement of QW_s distance at the lower frequencies specifically between 3 GHz and 5 GHz. With simulations, it is also found that any further extension in QW_m length results in poor resonance behavior, i.e., -10 dB bandwidth that is narrow and occurring outside the desired band of the antenna.

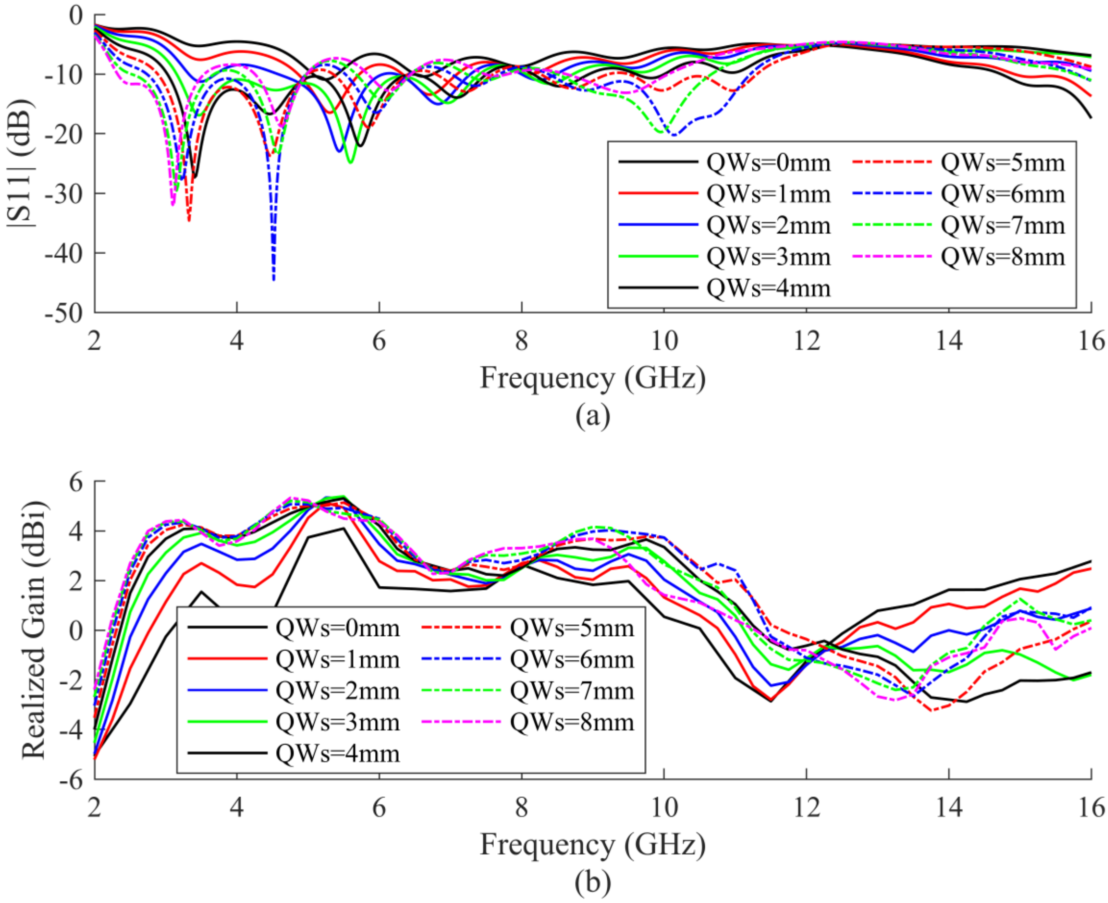

Figure 10. (a) Return loss and, (b) realized gain changes of the designed antenna with frequency calculated in the simulations over the band between 2 and 16 GHz for constant QW_m = 5 mm exceed length and different QW_s distances.

If we take a closer look at the -10 dB bandwidth of the antenna when parameters QW_s and QW_m are increased concurrently, one can observe that for the lower values of QW_m exceed length and QW_s distance, i.e. between 0 mm and 2 mm, the lower cutoff frequency of the antenna occurs at high frequencies as can be seen in Figure 11(a). As QW_m and QW_s parameters are further increased, both the lower cutoff frequency and the higher cutoff frequency shift towards lower frequencies. This is clearly seen in Figure 11(a) and 11(b). Furthermore, Figure 11(c) shows that the overall bandwidth of the antenna is mostly preserved for parameters QW_m and QW_s ranging between 2 mm and 4 mm. This indicates that one can design the antenna with the parameters provided in Table 1 while having some degree of freedom for tuning the operating bandwidth of the antenna based only on the total length of the micsrostrip feed and its latitudinal displacement along the linear slot.

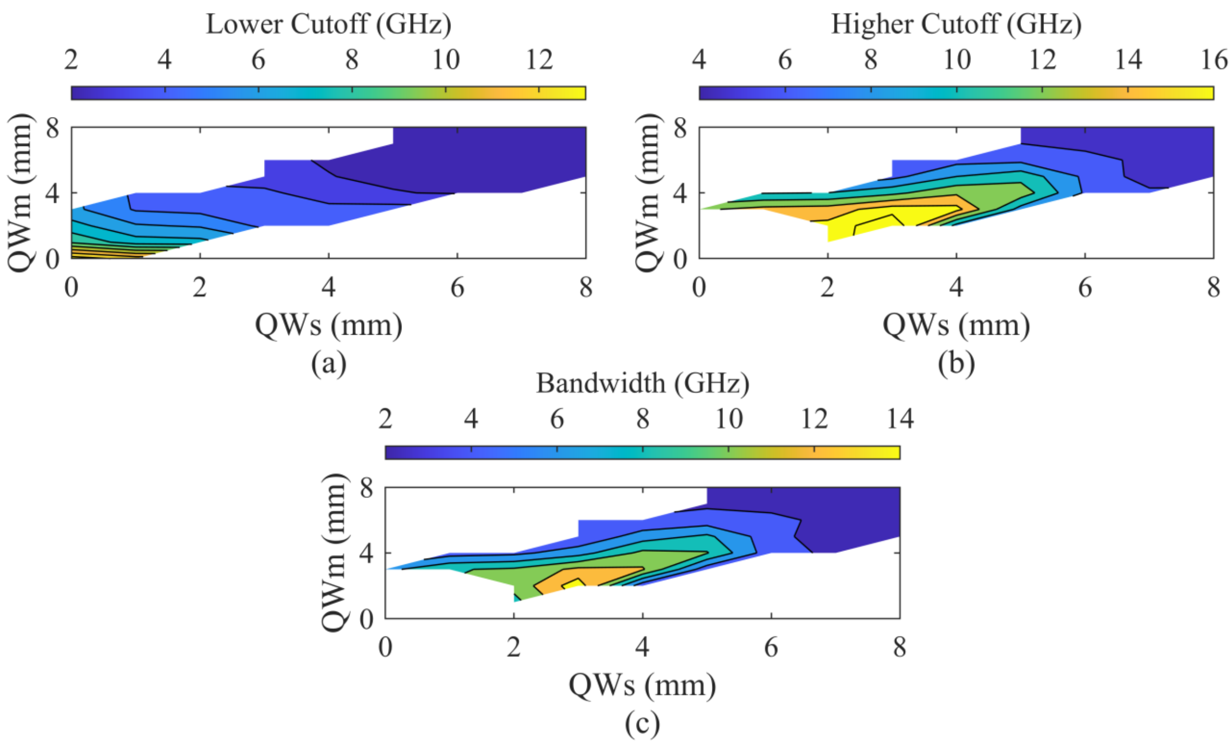

Figure 11. (a) Lower cutoff frequency, (b) higher cutoff frequency and, (c) bandwidth changes of the designed antenna for different QW_m exceed length and QW_s distances

4. Conclusion

In this paper, the design of a Vivaldi antenna with a -10 dB bandwidth between 3.1 to 13.6 GHz using a three-dimensional (3D) electromagnetic simulation tool was presented. A parametric study was then carried out to investigate the effect of the microstrip feed alignment on the antennas performance. In the simulations, the parameters QW_s and QW_m that correspond to the position of the feed network with respect to the linear slot start point and length of the feed exceeding the linear slot, respectively, were swept. Results show that as the feed network parameters vary between certain values the lower and higher cutoff frequencies of the antenna can be tuned while maintaining the total bandwidth. For the designed antenna, the total bandwidth of around 10 GHz is maintained as the QW_s parameter vary between 2 mm and 5 mm while the QW_m parameter change between 2 mm and 4 mm. This method may prove itself valuable for a variety of different UWB applications by allowing the designers to use the same geometrical antenna parameters and optimize the bandwidth for the desired frequencies with the alignment of the microstrip feed.

Statement of Conflict of Interest

The authors declare that there is no conflict of interest.

Author's Contributions

The authors declare that they have contributed equally to the article.

References

Allebes E., Singh G., He Y., Tiurin E., Mateman P., Ding M., Dijkhuis J., Schaik GJV., Bechthum E., Heuvel JVD., Soussi ME., Breeschoten A., Korpela H., Liu YH., Bachmann C. 21.2 A 3-to-10GHz 180pJ/b IEEE802.15.4z/4a IR-UWB coherent polar transmitter in 28nm CMOS with asynchronous amplitude pulse-shaping and injection-locked phase modulation. IEEE International Solid-State Circuits Conference (ISSCC) 2021; 304-306.

Breed G. A summary of FCC rules for ultra wideband communications. High Frequency Electronics 2005; 4(1): 42-44.

Chang DC. UWB antennas and their applications. 2008 International Workshop on Antenna Technology: Small Antennas and Novel Metamaterials 2008; 14-19.

Coburn W. Single layer vivaldi antenna feed analysis. 2019 International Applied Computational Electromagnetics Society Symposium (ACES) 2019; 1–2.

D'Amico S., De Matteis M., Rousseaux O., Philips K., Gyselinck B., Neirynck D., Baschirotto A. Ultra wide band in medical applications. Advances in Biomedical Sensing, Measurements, Instrumentation and Systems. Lecture Notes in Electrical Engineering, 55. Springer, Berlin, Heidelberg 2010; 43–60.

Federal Communications Commission. Ultra-wideband transmission systems. Federal Register 2002; 67(95): 34852–34860.

Gibson PJ. The vivaldi aerial. 1979 9th European Microwave Conference 1979; 101–105.

Hamzah N., Othman KA. Designing vivaldi antenna with various sizes using CST Software. Proceedings of the World Congress on Engineering 2011; 2.

Kahar M., Mandal J., Mandal MK. A compact vivaldi antenna with microstrip feed line for the 2-18GHz ultra-wideband applications. 2015 IEEE Applied Electromagnetics Conference (AEMC) 2015; 1–2.

Khusna EM., Setijadi E., Hendrantoro G. Parameter study of coplanar vivaldi antenna feeding structure. 2019 International Seminar on Intelligent Technology and Its Application (ISITIA) 2019; 13–18.

Kumar OP., Kumar P., Ali T., Kumar P., Vincent S. Ultrawideband antennas: Growth and evolution. Micromachines 2022; 13(1): 60.

Paulson CN., Chang JT., Romero CE., Watson J., Pearce FJ., Levin N. Ultra-wideband radar methods and techniques of medical sensing and imaging. Proc. SPIE 6007, Smart Medical and Biomedical Sensor Technology III 2005.

Rana MM., Khanom R., Rahman MM. Design and analysis of vivaldi antennas. 2018 International Conference on Innovation in Engineering and Technology (ICIET) 2018; 1–5.

Saeidi T., Ismail I., Wen WP., Alhawari ARH., Mohammadi A. Ultra-wideband antennas for wireless communication applications. International Journal of Antennas and Propagation 2019; 4: 7918765-1–7918765-25.

Shafieha JH., Noorinia J., Ghobadi C. Probing the feed line parameters in vivaldi notch antennas. Progress In Electromagnetics Research B (2008); 1: 237–252.

Shantz HG. The art and science of ultrawideband antennas (second edition). Artech House 2015.

Singh A., Nair T., Roy S., Srivastava A., Verma V. Design and testing of vivaldi antenna for UWB applications. 2023 2nd International Conference on Vision Towards Emerging Trends in Communication and Networking Technologies (ViTECoN) 2023; 1–5.

Singh G., Allebes E., He Y., Tiurin E., Mateman P., Dijkhuis JF., Schaik GJV., Bechthum E., Heuvel JVD., Soussi ME., Breeschoten A., Korpela H., Gordebeke GJ., Lemey S., Bachmann C., Liu YH. An IR-UWB IEEE 802.15.4z compatible coherent asynchronous polar transmitter in 28-nm CMOS. IEEE Journal of Solid-State Circuits (2021); 56(12): 3799–3810.

Song M., Allebes E., Marshall C., Bhat AN., Bechthum E., Dijkhuis J., Traferro S., Tiurin E., Vis P., Heuvel JVD., Soussi ME., Boer P., Sheikh A., Meyer B., Liu J., Ven SVD., Winkel N., Hijdra M., Ramachandra GK., Baykal Y., Visser H., Zhang P., Breeschoten A., Liu YH., Bachmann C. An 8.7 mW/TX, 21 mW/RX 6-to-9GHz IEEE 802.15.4a/4z compliant IR-UWB transceiver with pulse pre-emphasis achieving 14mm ranging precision. 2023 IEEE Symposium on VLSI Technology and Circuits (VLSI Technology and Circuits) 2023; 1–2.

Valderas D., Sancho JI., Puente D., Ling C., Chen X. Ultrawideband antennas: Design and applications. Imperial College Press 2010.